Marcin, W.; Benedito, A.; Giménez Torres, E. (2014). Preparation and Characterization of Extruded Nanocomposite Based on Polycarbonate/Butadiene-Acrylonitrile-Styrene Blend Filled with Multiwalled Carbon Nanotubes. Journal of Applied Polymer Science. 131(10). https://doi.org/10.1002/app.40271

Preparation and characterization of extruded nanocomposite based on \polycarbonate/butadiene-acrylonitrile-styrene blend filled with multi-walled carbon nanotubes.

Wegrzyn Marcin[1], Adolfo Benedito[1], Enrique Gimenez[2]*

[1] Instituto Tecnológico del Plástico (AIMPLAS), Calle Gustave Eiffel 4, 46980 Paterna, Spain

[2] Instituto de Tecnología de Materiales. Universidad Politécnica de Valencia, Camino de Vera, 46022 Valencia, Spain

Correspondence: e-mail: marcinwegrzyn@hotmail.com, tel.: (+34) 671213870

Abstract:

In this work, nanocomposites of polycarbonate/acrylonitrile-butadiene-styrene (PC/ABS) with multi-wall carbon nanotubes (MWCNT) were prepared by pre-dispersed masterbatch dilution. Melt compounding on a twin screw extruder was followed by characterization of rheological, mechanical, thermal and morphological properties of the nanocomposites influenced by MWCNT concentration.

Light-transmission- and scanning electron microscopy supported by Raman spectroscopy showed preferential location of MWCNT in polycarbonate. Nevertheless, relatively good dispersion in the whole matrix was achieved. Specific mechanical energy calculated for nanocomposite system was higher at lower processing temperature. Thermal stability was investigated by TGA while transition temperatures by DSC. Study of viscoelastic properties of PC/ABS-MWCNT showed the fluid–solid transition below 0.5 wt.% MWCNT. Beyond this point continuous nanofiller network is formed in the matrix promoting the reinforcement. Addition of 0.5 wt.% MWCNT reduced ductility of PC/ABS and enhanced Young's modulus by *c.a.* 30% and yield stress by *c.a.* 20%. Moreover, theoretical values of stiffness calculated within this work agree with the experimental data. Boosted electrical properties, showing percolation at 2.0 wt.% MWCNT, are influenced by melt temperature during extrusion.

These results reveal that the preparation of PC/ABS nanocomposites from masterbatch dilution is an excellent method to obtain well-dispersed MWCNT and a good balance of electrical and mechanical properties.

Keywords: A. Polymer-matrix composites (PMCs), B. Mechanical properties,
C. Thermal analysis, Nanocomposites

1. **Introduction**:

Miscible- and multiphase polymer blends create over 36% of polymer production industry [1]. Development of nanocomposites based on such matrix filled with multi-walled carbon nanotubes (MWCNT) offer novel possibilities to produce materials with tailored properties. Both: miscible [2] and immiscible [3-4] blends exhibit desired performance characteristics after incorporation of MWCNT. Carbon nanotubes characterized by unique structure and uncommon properties have already reached an important position in science and technology. High aspect ratio causes the boost of electrical- and thermal conductivity in isolating polymers at relatively low loads [5-6]. Likewise, shape and properties of MWCNT allow improving mechanical properties of polymer matrix when homogeneous dispersion is achieved. This is related to the mechanical percolation based on interactions between carbon nanotubes and polymer chains [7]. Nevertheless, achieving of good dispersion of carbon nanotubes in polymers by melt-mixing is one of the key challenges. Agglomeration level based on attractive Van der Waals forces between individual nanotubes appears to be tunable when twin-screw extrusion is applied [8]. Tailoring the key processing parameters during nanocomposite preparation and further processing [9] allows significant decrease of agglomeration and control of alignment in the final part [10]. Specific mechanical energy (SME) is recognized parameter describing energy applied to the material during melt mixing [11]. Proper control of the compounding process and selection of correct processing parameters, in particular with the design of screw profile, is a significant factor in the quality of the final nanocomposite [8]. There are some literature examples of melt-mixed nanocomposites of carbon nanotubes in commodity polymers, such as polyethylene (PE) [12], polypropylene (PP) [13] or polystyrene (PS) [14]. Materials based on engineering plastics such as polycarbonate (PC) have attracted considerable interest in recent years. Alig *et al.* [15] reported strong dependence between electrical conductivity, MWCNT content and processing parameters for nanocomposites based on polycarbonate (PC). The destruction of nanofiller network and, thus a decrease of electrical conductivity was reported when a high screw speed was used. *Primary*- and *secondary agglomeration* theory explains nanofiller bundling what is related to electrical conductivity reinforcement in plastics [6]. Presence of tightly packed agglomerates in the nanofiller before extrusion makes de-agglomeration more difficult and, thus decreases the homogeneity of MWCNT dispersion.

However, it is claimed that the size on carbon macro-structures can be modified with changed shear conditions, *e.g.* with ball mill treatment of nanotubes before further processing [16]. Proper parameters (high screw speed, low barrel temperature) guarantee better dispersion, so increased contact between the individual nanotubes and matrix.

PC/ABS blends filled with carbon nanotubes were studied by Xiong *et al.* [3] and Sun *et al.* [4]. In both cases blends were prepared by researchers form the neat components and migration or controlled location of MWCNT was reported. Besides, affinity of carbon nanotubes to polycarbonate component at defined PC-to-ABS ratio was explained showing the challenge of achieving a uniform distribution of MWCNT in both components when commercial PC/ABS blends are used.

In this work we present PC/ABS-MWCNT nanocomposites prepared by pre-dispersed masterbatch dilution on twin-screw extruder at two temperatures. Specific mechanical energy (SME) applied to the material during processing is discussed. Morphology is characterized by light-transmission- (OM), scanning electron microscopy (SEM) and Raman spectroscopy. Thermal properties are investigated by thermo-gravimetric analyses (TGA), differential scanning calorimetry (DSC) while mechanical properties by dynamic-mechanical analysis (DMA) and tensile testing. Moreover, theoretical predictions of mechanical improvement are correlated with the experimental data.

2. **Materials and Experimental Procedure**:

Commercial blend of polycarbonate and acrylonitrile-butadiene-styrene (PC/ABS) Bayblend® T85, supplied by Bayer MaterialScience, contains 85 wt.% of polycarbonate. MVR is 12 cm^3/10 min, Vicat softening temperature is 129ºC (data provided by supplier). Multi-walled carbon nanotubes (MWCNT) NC7000 are supplied by Nanocyl. Average diameter is 9.5 nm and average length 1.5 μm (data provided by supplier).

Nanocomposites were obtained with a throughput of 1 kg h^{-1} on the twin-screw co-rotating laboratory extruder Prism Eurolab 16 (Thermo Fisher Scientific) of length-to-diameter ratio (L/D) 25. Screw profile was designed using Ludovic software (Sciences Computers Consultants). Nanocomposites are produced at 260ºC or 280ºC with screw speed 400rpm. Carbon nanotubes were fed to the extruder with a pneumatic feeder (Brabender Technologies) together with PC/ABS pellets. Final nanocomposites were subsequently formed by dilution of 5.0 wt. % MWCNT masterbatch (prepared in the same conditions as dilution) to concentrations between 0.5 wt. % and 3.0 wt.

%. PC/ABS pellets and masterbatch pellets were dried in vacuum at 100°C for 4h before each processing stage. Rectangular samples with dimensions of 60x10x2 mm^3 following modified standard ISO 127 were compression molded on Collin 6300 hydraulic press at 260 ºC in order to be used for thermo-mechanical tests and electrical conductivity measurements. Additionally, dog-bone specimens following standard ISO 527-3 were obtained at the same conditions for the use in evaluation of mechanical properties.

Morphology of the nanocomposites was studied by light-transmission microscopy (OM) on Leica DMRX microscope and by scanning electron microscopy (SEM) on JEOL 7001F scanning electron microscope. Films 20-50 μm thick for OM study were heat-pressed from pellets. SEM samples were platinum-coated using a sputtering device Baltec SCMCS010. Raman spectroscopy measurements were done on Horiba XploRA with 532nm laser LCM-S-11 and CCD detector.

Thermo-gravimetric analysis (TGA) was done on Q5000 instrument (TA Instruments). Pellets were heated from 50°C to 600°C at a heating rate of 20°C min^{-1} under nitrogen atmosphere. Differential scanning calorimetry (DSC) was done on Diamond (Perkin-Elmer). Each sample was heated from 40ºC to 280ºC with a heating rate of 10ºCmin^{-1} to erase the thermal history. This was followed by cooling to 40ºC at the same conditions and second heating to 280ºC in order to determine the glass transition temperature and enthalpies.

Viscoelastic properties of nanocomposites were investigated on AR G2 rotational rheometer (TA Instruments) with parallel plate geometry (diameter 25mm) at 280ºC. Strain was set to 1% according to the results of strain sweep. Dynamic mechanical analysis (DMA) was done on DMA-2980 (TA Instruments) with dual cantilever clamp at vibration frequency 1 Hz, temperature range from 35°C and 200°C and scan rate of 3°Cmin^{-1}. Tensile testing was performed according to ASTM D-638 on an Instron Universal Machine 3343 with 5kN load cell and 5mm min^{-1} extension velocity. Experiments were done at constant conditions: 50±5% HR and 24±2ºC.

Electrical resistivity was measured by twp-point contact configuration following ISO 3915 standard on Keithley 2000 Multimeter source/meter. Silver electrodes were painted on the samples in order to improve contact with measuring electrodes.

3. **Results and Discussion**:

3.1. **Morphology**

Morphology of nanocomposite obtained by melt mixing immiscible PC/ABS blend with carbon nanotubes is present on OM images in Figure 1. Relatively good dispersion of MWCNT with minor agglomeration is achieved for all applied processing conditions showing little difference between low and high barrels temperature. Nanocomposites prepared at 260 ºC show more homogeneous morphology than those produced at 280ºC. This difference is clear at higher MWCNT loads. Moreover, at 260 ºC the reduction of agglomerates quantity per controlled area appears along with the increase of agglomerate size with the change of nanofiller load from 1.0 wt.% to 3.0 wt.%. Such agglomeration behavior can be correlated with specific mechanical energy (SME) curves shown in Figure 2 and calculated with Equation (1). This important parameter characterizing process by showing effectivity of the selected conditions includes εP as the effective power of motor, τ representing torque and Q - throughput. Input data contains also screw speed ratio between the applied (v_{proc}) and the maximum (v_{max}) value. Throughput Q was constant for all experiments in order to facilitate results analyses. However, reports regarding influence of that parameter exist in the literature [11]. Therefore, SME understood as a relation between various mutually correlated parameters is directly proportional to torque (influenced by melt viscosity) and to screw speed [17]. Clear dependence of SME on melt temperature and MWCNT load is present in Figure 2. Higher values of shear applied at lower temperature show clear increase of SME. This behavior can be derived from higher viscosity at lower temperatures and higher MWCNT loads. Sufficient mixing energy gives possibility to obtain relatively good dispersion of carbon nanotubes [11].

Previous reports on PC/ABS investigation allows to define the immiscible phases in SEM micrographs [18]. Morphology of nanocomposites studied on SEM micrographs shows preferential location of carbon nanotubes in polycarbonate, appearing as

a smooth surface, rather than in ABS (Figure 3). This situation does not change with an increase of MWCNT load or at various processing conditions. These conclusions can be correlated with the calculations of surface energies and wetting coefficient between MWCNT and matrix components [19-20]. The interfacial tension obtained from partial surface tensions between the defined phases of the blend show that carbon nanotubes have significantly higher affinity to PC, what agrees with the observations. Moreover, agglomeration behavior expected at higher carbon nanotubes loads is present in SEM micrographs. Figure 3b shows entangled and individual MWCNT, while for lower nanofiller concentration mainly well-dispersed structures are present.

Vibrational spectra of PC/ABS present in Figure 4 shows the characteristic pattern between 600 cm^{-1} and 2000 cm^{-1}. The Raman bands at 1880 cm^{-1}, 1112 cm^{-1} and 885 cm^{-1} are representing C-H in-plane and out-of-plane wagging modes. Broad band between 1200 cm^{-1} and 600 cm^{-1} are related to C-O stretching and C-H deformation [21]. Characteristic bands for pristine multi-walled carbon nanotubes appear at 1340 cm^{-1} and 1575 cm^{-1} for D-band and G-band, respectively [21]. For nanocomposites the bands are shifted towards the higher wave-number (blue shift) showing the positions at *c.a.* 1347 cm^{-1} and *c.a.* 1599 cm^{-1} for D- and G-band, respectively. This effect is explained as results of MWCNT disentanglement and has been reported earlier [22]. Besides the band at *c.a.* 1500 cm^{-1} overlaps with the G-band of multi-walled carbon nanotubes, what makes the intensities ratio of characteristic bands (D/G) more effective parameter. In this regard the decrease of D/G was observed from 0.99±0.01 for MWCNT to 0.95±0.01 for PC/ABS with 1.0 wt.% MWCNT. This can be related to the local stress between MWCNT and the polymer [23-24] represented by the mechanical compression transferred from the matrix to MWCNT [25].

3.2. **Thermal properties**

Figure 5 shows thermal degradation behavior of pristine PC/ABS and selected nanocomposites measured by TGA. Both components of the matrix can be distinguished by two-step decomposition. Moreover, the initial part of the curve (*c.a.* 400ºC-475ºC) representing degradation of ABS shows slight increase of thermal stability after the incorporation of carbon nanotubes. Even though polycarbonate seems to show no significant change after the formation of nanocomposite, results present in Table 1 show similar trend for both blend components. Furthermore, only slight increase of thermal stability for polycarbonate was observed with an increase of carbon nanotubes load. This behavior of decreased thermal stability with an incorporation of carbon nanotubes to polymer matrix, has been reported earlier [26]. Impurities in nanofiller (e.g. metal ions) can act as Lewis acids weakening radicals and causing easier thermal degradation.

Table 1 shows the DSC results: glass transition temperature (T_g) and change of heat capacity at glass transition temperature (ΔC_p) for investigated nanocomposites. The trend is opposite for both PC/ABS phases. Chain mobility basing on interactions between well-dispersed individual carbon nanotubes and polymer chains can be investigated rather with the heat capacity [27]. The network of carbon nanotubes reduces freedom degree of polymer chains, what should cause the decrease of ΔC_p. This effect occurs for ABS phase with only reduced amount of MWCNT. However, with the increase of carbon nanotube load,

morphology evolution can occur locating more nanofiller in ABS. This was described by Xiong *et al.* [3] as an effect related to processing conditions. Nevertheless, such phenomenon can also be related to the increase of carbon nanotubes content. On the contrary, agglomeration in PC increasing at higher nanofiller load provides higher mobility of polymer chains what affects the change of heat capacity at glass transition temperature.

3.3. **Rheology**

Rheology of PC/ABS-MWCNT nanocomposites in Figure 6 shows clear dependence of carbon nanotubes load. An increase of storage modulus (G') with the increase of MWCNT load is observed. Moreover, all investigated nanocomposites show solid-like behavior with rubber plateau at high angular frequency. Such plateau is more obvious at higher nanofiller loads and can be observed above defined molecular carbon nanotube-polymer chain entanglement [7]. The transition between liquid- and solid-like behavior is also related to molecular weight of polymer chains that are clearly reduced after processing and is expected below 0.5 wt.% [28]. Such rheological percolation is believed to base on combined nanotubes-polymer network rather than exclusively on MWCNT network (as it appears for electrical percolation threshold) [7]. Disentanglement of such structure is more difficult than disentanglement of polymer-polymer network at low frequencies. Substantial influence of carbon nanotubes on the polymer relaxation dynamics is explanation of material behavior observed on linear viscoelastic properties at low MWCNT loads and low frequencies [29]. On the other hand, higher MWCNT loads provide better interconnection between polymeric chains resulting with aforementioned rubber plateau.

3.4. **Mechanical Properties**

Tan δ, defined as the ratio of loss modulus to storage modulus, is a measure of inherent material damping (energy dissipation). Figure 7 shows the value of the Tan δ (maximum peak) according to the incorporation of the MWCNT into PC/ABS matrix. An increase of tan δ with increase of carbon nanotube load is observed for both matrix components. Nevertheless, the improvement is higher in the mayor phase (PC) than minor phase (ABS) Increase of the transition temperature in both phases indicates improvement of mechanical properties. The above observations can be correlated with these results regarding tan δ as cross-linking sensitive parameter. Higher carbon nanotubes concentrations create more entanglements

between polymer chains that can be understood as a formation of such network influencing energy absorption.

Carbon nanotubes content influence on Young's modulus is shown in Figure 8. Significant improvement of stiffness is achieved after introduction of 0.5 wt.% MWCNT. Further increase of nanofiller concentration gives rather minor change of Young's modulus. Nevertheless, Table 2 shows an increase of yield stress and a decrease of elongation at break at higher carbon nanotube loads. This behavior is expected and has been observed by other authors [30]. Different trend in Young's modulus below and above 0.5 wt.% can be related to higher agglomeration at higher loads. In this regard, change of load transfer mechanism can be considered to explain such decrease of ductility at elevated carbon nanotube loads.

Comparison of experimental data of PC/ABS nanocomposites with theoretical model based on Halpin-Tsai equations [31] is shown in Figure 8. Reported modifications of this method, originally related to micro-fillers, broaden its application range to nanocomposites [32-34]. Theoretical values of Young's modulus calculated with Equation (2) agree with experimental data in the whole MWCNT concentration range. Factor η described by Equation (3) defines the efficiency of the nanofiller while ζ, Equation (4), is related to the geometry and the boundary conditions of the reinforcement of the individual nanotube. Young's modulus of nanofiller (E_f) and PC/ABS (E_m) are 980 GPa and 1.2 GPa respectively. MWCNT load is defined by volume fraction (V_f). However, rather poor agreement between theoretical and experimental data is achieved with classic Halpin-Tsai model. Correct orientation factor α, experimental k_A factor and waviness coefficient K_ω need to be selected to improve this, especially for higher carbon nanotube loads. According to the literature α value 0.17 represents randomly oriented MWCNT, so the situation expected in this study [32]. Waviness coefficient ranges usually between 0 and 1, and represents the share of force transferred by MWCNT along the central axis. Even though non-modified calculation method does not fit the experimental data independently on waviness coefficient, non-modified method seems to agree with nanocomposite below 0.5 wt.% MWCNT when higher share of long axes of the nanotubes is considered (K_ω 0.2). Besides, correct experimental curves fitting with theory occurs when non-linear dependence between carbon nanotubes load and mechanical performance is defined.

3.5. **Electrical properties**

Figure 9 shows electrical conductivity of nanocomposites obtained at various temperatures. Conductivity of neat PC/ABS, e^{-15} Scm^{-1}, is boosted *c.a.* fourteen orders of magnitude with the load of 1.0 wt.% MWCNT. Rapid improvement of electrical properties with an increase of nanofiller content occurs above 2.0 wt.% marking percolation threshold. However, only minor difference can be observed with the change of melt temperature (between 260ºC and 280ºC). In both cases electrical percolation (Φ_e) is present at almost exactly equal concentration. Besides, mechanical percolation observed in flow curves occurs at clearly lower loads than conductive network is formed. This can be related to different character of both networks, regarding polymer chains-nanotubes network in the latter case [7,28-29]. Electrical conductivity demands nanotube-nanotube direct contacts or very little distances to provide charge path between the electrodes. Furthermore, immiscible blends show double percolation phenomenon based on the continuity of conductive filler-rich phase in the other phase of the matrix. Furthermore, electrical conductivity varies almost an order of magnitude between 2.0 wt.% and 3.0 wt.%, what is rather uncommon behavior after percolation point.

4. **Conclusions**

In this work we present result of characterization of PC/ABS-MWCNT nanocomposite processed by melt-mixing. Specific mechanical energy is found to show clear difference favoring lower processing temperatures. Commercial, immiscible blend forms nanocomposites of good morphology with majority of nanofiller located in polycarbonate. This agrees with the literature calculations basing on surface energies of blend components. The dilution of pre-dispersed masterbatch on twin-screw extruder result with the improvement of thermal-, mechanical- and electrical properties. Thermal properties are related to the dispersion of MWCNT in polymer matrix. Change of heat capacity at glass transition temperature indicates the increase of carbon nanotube content in ABS phase at elevated loads. Besides, mechanical percolation estimated on storage modulus (*G'*) curves appears to be significantly lower than electrical percolation, indicating relative difficulty in achievement of conductive path in commercial PC/ABS and the presence of MWCNT-rich phase. Mechanical properties improved with MWCNT load shows acceptable fitting with theoretical values calculated with modified Halpin-Tsai method.

Balance between mechanical- and electrical- properties observed during this work creates an attractive opportunity for automotive- and electronic industries. Applicability of these nanocomposites by injection molding of PC/ABS-MWCNT nanocomposites will be presented in a future work.

Acknowledgement

This work is funded by the European Community's Seventh Framework Program (FP7-PEOPLE-ITN-2008) within the CONTACT project Marie Curie Fellowship under grant number 238363.

References

[1] Göldel A., Pötschke P.: Carbon nanotubes in multiphase polymer blends. in 'Polymer-carbon nanotube composites' (eds.: McNally T., Pötschke P.) Woodhead Publishing, Oxford, Vol 1, 587-620 (2011).

[2] Sathyanarayana S., Wegrzyn M., Olowojoba G., Benedito A., Gimenez E., Hübner C., Henning F.: Multiwalled carbon nanotubes incorporated into a miscible blend of poly(phenyleneether)/polystyrene – processing and characterization, Express Polymer Letters, 7, 621-635 (2013).
DOI: 10.3144/expresspolymlett.2013.59.

[3] Xiong Z.Y., Wang L., Sun Y., Guo Z.X., Jian Y.: Migration of MWCNTs during melt preparation of ABS/PC/MWCNT conductive composites via PC/MWCNT masterbatch approach, Polymer, 54, 447-455 (2013).
DOI: 10.1016/l.polymer.2012.11.044.

[4] Sun Y., Gou Z.X., Yu J.: Effect of ABS rubber content on the localization of MWCNT in PC/ABS blends and electrical resistivity of the composites, Macromolecular Materials and Engineering, 295, 263-268 (2010).
DOI: 10.1002/mame.200900242.

[5] Yang L., Liu F., Xia H., Qian X., Shen K., Zhang J.: Improving the electrical conductivity of a carbon nanotube/polypropylene composite by vibration during injection molding, Carbon, 49, 3274-3283 (2011).
DOI: 10.1016/j.carbon.211.03.054.0

[6] Pötschke P., Dudkin S.M., Alig I.: Dielectric spectroscopy on melt-processed polycarbonate-multiwalled carbon nanotube composites, Polymer, 44, 5023-5030 (2003).
DOI: 10.1016/S0032-3861(03)00451-8.

[7] Pötschke P., Abdel-Goad M., Alig I., Dudkin S., Lellinger D.: Rheological and dielectrical characterization of melt mixed polycarbonate-multiwalled carbon nanotube composites. Polymer, 45, 8863-8870 (2004).

DOI: 10.1016/j.polymer.2004.10.040.

[8] Villmow T., Kretzschmar B., Pötschke P.: Influence of screw configuration, residence time, and specific mechanical energy in twin-screw extrusion of polycaprolactone/multi-walled carbon nanotube composites, Composite Science and Technology, 70, 2045-2055 (2010).

DOI: 10.1016/j.compscitech.2010.07.021.

[9] Villmow T, Pegel S, Pötschke P, Wagenknecht U.: Influence of injection molding on the electrical resistivity of polycarbonate filled with multi-walled carbon nanotubes, Composite Science and Technology, 68, 777-789 (2008).

DOI: 10.1016/j.compscitech.2007.08.031.

[10] Duong H.M., Tamamoto N., Bui K., Papavassiliou D.V., Maruyama S., Wardle B.L.: Morphologic effects on non-isotropic thermal conduction of aligned single- and multi-walled carbon nanotubes in polymer nanocomposites, Journal of Physical Chemistry C, 114, 8851-8860 (2010).

DOI: 10.1021/jp102138c.

[11] Sathyanarayana S., Olowojoba G., Weiss P., Calgar B., Pataki B., Mikonsaari I., Huebner C., Hening F.: Compounding of MWCNTs with PS in a twin-screw extruder with varying process parameters: morphology, interfacial behavior, thermal stability, rheology, and volume resistivity. Macromolecular Materials and Engineering, 298, 89-105 (2013).

DOI: 10.1002/mame.201200018

[12] Vega J.F., Martinez-Salazar J., Trujillo M., Arnal M.L., Müller A.J., Bredeau S., Dubois P.: Rheology, processing, tensile properties and crystallization of polyethylene/carbon nanotube nanocomposites, Macromolecules, 42, 4719-4727 (2009).

DOI: 10.1021/ma900645f.

[13] Alig I., Lellinger D., Dudkin S., Pötschke P.: Conductivity spectroscopy on melt processed polypropylene-multiwalled carbon nanotube composites: recovery after shear and crystallization, Polymer, 49, 1020-1029 (2007).

DOI: 10.1016/j.polymer.2006.12.035.

[14] Hill D.E., Lin Y., Rao A.M., Allard L.F., Sun Y.P.: Functionalization of carbon nanotubes with polystyrene, Macromolecules, 35, 9466-9471 (2002).

DOI: 10.1021/ma020855r.

[15] Alig I., Lellinger D., Engel E., Skipa T., Pötschke P.: Destruction and formation of a conductive carbon nanotube network in polymer melts: in-line experiments, Polymer, 49, 1902-1909 (2008).
DOI: 10.1016/j.polymer.2008.01.073.

[16] Krause B., Villmow T., Boldt R., Mende M., Petzold G., Pötschke P.: Influence of dry grinding in a ball mill on the length of multiwall carbon nanotubes and their dispersion and percolation behavior in melt mixed polycarbonate composites, Composites Science and Technology, 71, 1145-1153 (2011).
DOI: 10.1016/j.compscitech.2011.04.004.

[17] Krause B., Pötschke P., Häußler L.: Influence of small scale melt mixing conditions on electrical resistivity of carbon nanotube-polyamide composites. Composite Science and Technology, **69**, 1505-1515 (2009).
DOI: 10.1016/l.composcitech.2008.07.007

[18] Krache R., Debbah I.: Some mechanical and thermal properties of PC/ABS blends. Materials Science and Application, 2, 404-140 (2011).
DOI: 10.4236/msa.2011.25052

[19] Nuriel S., Liu L., Barber A.H., Wagner H.D.: Direct measurement of carbon nanotube surface tension. Chemical Physics Letters, 404, 263-265 (2005).
DOI: 10.1016/j.cplett.2005.01.072

[20] Barber A.H., Cohen S.R., Wagner H.D.: Static and dynamic wetting measurements of single carbon nanotubes. Physical Review Letters, 92, 186103(4).
DOI: 10.1103/PhysRevLett.92.186103

[21] Ahmed S.F., Ji J.W., Moon M.W., Jang Y.J., Park B.H., Lee S.H.: The morphology and mechanical properties of polycarbonate/acrylonitrile butadiene styrene modified by Ar ion beam radiation. Plasma Processes and Polymers, 6, 860-865 (2009).
DOI: 10.1002/ppap.200900043

[22] Bokobza L., Zhang J.: Raman spectroscopic characterization of multiwall carbon nanotubes and of nanocomposites, Express Polymer Letters, 6, 601-608 (2012).
DOI: 10.3144/expresspolymlett.2012.63.

[23] Deng L., Eichhorn S.J., Kao C.C., Young R.J.: The effective Young's modulus of carbon nanotubes in composites. ACS Applied Material Interfaces, 3, 433-440 (2011).
DOI: 10.1021/am1010145.

[24] Cooper C.A., Young R.J., Halsall M.: Investigation into the deformation of carbon nanotubes and their composites through the use if Raman spectroscopy. Composites Part A: Applied Science and Manufacturing, 32, 401-411 (2001).
DOI: 10.1016/S1359-835X(00)00107-X

[25] Yan X., Itoh Y., Kitahama Y., Suzuki T., Sato H., Miyake T., Ozaki Y.: A Raman Spectroscopy Study on Single-Wall Carbon Nanotube/Polystyrene Nanocomposites: Mechanical Compression Transferred from the Polymer to Single Wall Carbon Nanotubes. The Journal of Physical Chemistry C, 116, 17897-17903 (2012).
DOI: 10.1021/jp303509g

[26] Schartel B., Braun U., Knoll U., Bartholmai M., Goering H., Neubert D., Pötschke P.: Mechanical, thermal and fire behavior of bisphenol A polycarbonate/multiwall carbon nanotubes, Polymer Engineering and Science, 48, 149-158 (2008).
DOI: 10.1002/pen..20932.

[27] Su S.P., Xu Y.H., Wilkie C.A.: Thermal degradation of polymer-carbon nanotube composites. in 'Polymer-carbon nanotube composites' (eds.: McNally T., Pötschke P.) Woodhead Publishing, Oxford, Vol 1, 482-510 (2011).

[28] Abdel-Goad M., Pötschke P.: Rheological characterization of melt processed polycarbonate-multiwalled carbon nanotube composites. Journal of Non-Newtonian Fluids Mechanics, 128, 2-6 (2005).
DOI: 10.1016/j.jnnfm.2005.01.008.

[29] Du F., Scogna R.C., Zhou W., Brand S., Fischer J.E., Winey K.I.: Nanotube networks in polymer nanocomposites: rheology and electrical conductivity. Macromolecules, 37, 9048-9055 (2004).
DOI: 10.1021/ma049164g.

[30] Abbasi S., Carreau P.J., Derdouri A.: Flow induced orientation of multiwalled carbon nanotubes in polycarbonate nanocomposites: rheology, conductivity and mechanical properties, Polymer, 51, 922-935 (2010).
DOI: 10.1016/j.polymer.2009.12.041.

[31] Halpin J.C., Kardos J.L.: Halpin-Tsai equatons: a review. Polymer Engineering and Science, 16, 344-352 (1976).
DOI: 10.1002/pen.760160512.

[32] Arasteh R., Omidi M. Rousta A.H.A., Kazerooni H.: A study on effect of waviness of mechanical properties of multi-walled carbon nanotube/epoxy composites using Halpin-Tsai theory. Journal of Macromolecular Science, Part B. Physics, 50, 2464-2480 (2011).
DOI: 10.1080/00222348.2011.579868.

[33] Srivastava V.K., Singh S.: A micro-mechanical model of elastic modulus of multi walled carbon nanotube/epoxy resin composites, International Journal of Composite Materials, 2, 2-6 (2012).
DOI: 10.5923/j.cmaterials.20120202.01.

[34] Jiang Z., Hornsby P., McCool R., Murphy A.: Mechanical and thermal properties of polyphenylene sulfide/multiwalled carbon nanotube composites, 123, 2676-2683 (2012).
DOI: 10.1002/app.34669.

Figure captions

Figure 1: Light-transmission microscopy images of PC/ABS-MWCNT nanocomposite processed at 260ºC: a) 1.0 wt. %, b) 3.0 wt. %, and 280ºC: c) 1.0 wt. %, d) 3.0 wt. %.

Figure 2: Specific mechanical energy of PC/ABS-MWCNT nanocomposites extruded at various temperatures.

Figure 3: SEM micrographs of PC/ABS-MWCNT nanocomposite processed at 260ºC: a) 1.5 wt. %, b) 3.0 wt. % with circled agglomerate.

Figure 4: Raman spectra of PC/ABS, MWCNT and resulting nanocomposite (1.0 wt.%).

Figure 5: Thermal degradation curves for pristine matrix and two selected nanocomposites.

Figure 6: Storage modulus of neat and processed PC/ABS and of its selected nanocomposites with MWCNT.

Figure 7: Dynamic mechanical analyses results for PC/ABS and its nanocomposites with MWCNT.

Figure 8: Young's modulus dependence of MWCNT load in PC/ABS-MWCNT nanocomposites compared with theoretical data.

Figure 9: Electrical conductivity of PC/ABS processed at different barrels temperature.

Table captions

Table 1: Thermal properties of PC/ABS nanocomposites processed at 260 ºC .

Table 2: Mechanical properties of PC/ABS nanocomposites processed at 260 ºC.

Equations:

(1) $$SME = \frac{\varepsilon P \cdot \tau \cdot \frac{v_{proc}}{v_{\max}}}{Q}$$

(2) $$E_{nc} = k_A \frac{1+\zeta\eta V_{CNT}}{1-\eta V_{CNT}} E_m$$

(3) $$\eta = \frac{K_\omega\left(\alpha \frac{E_f}{E_m}\right)-1}{K_\omega\left(\alpha \frac{E_f}{E_m}\right)-\zeta}$$

(4) $$\zeta = \frac{2l}{d}$$

Figures

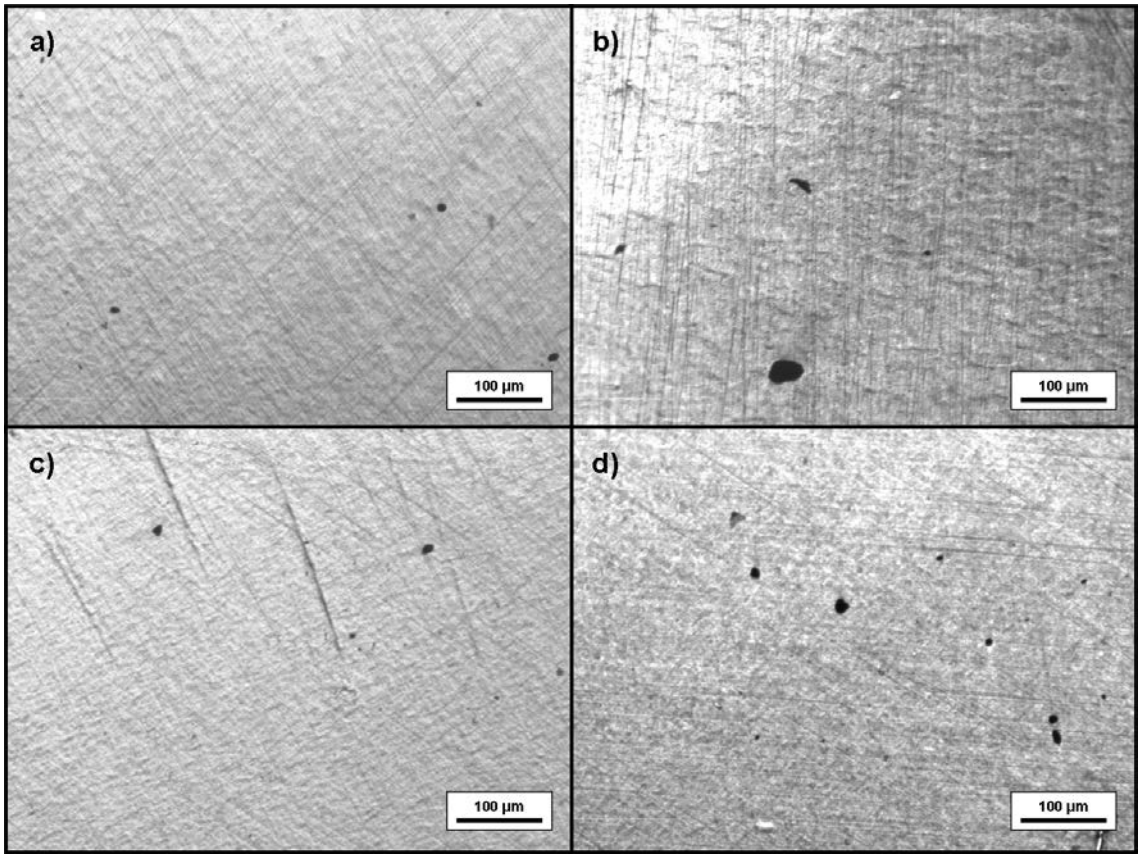

Figure 1.

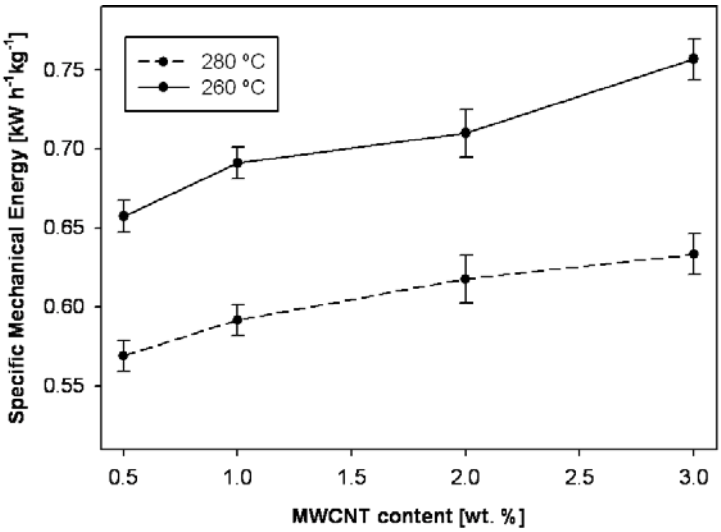

Figure 2.

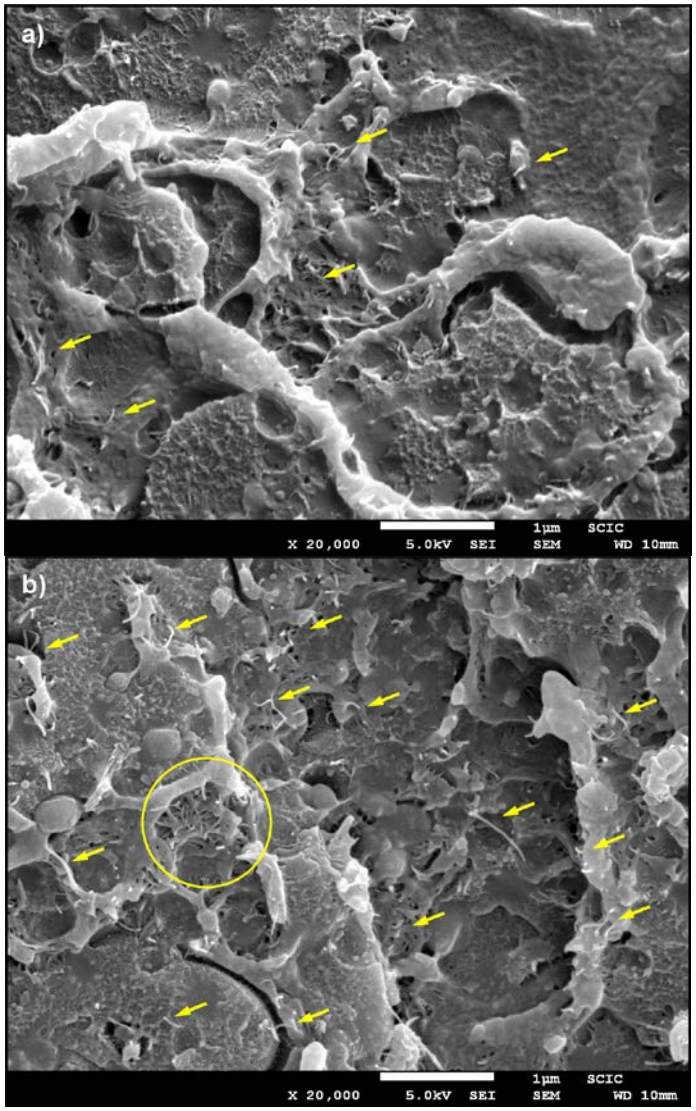

Figure 3.

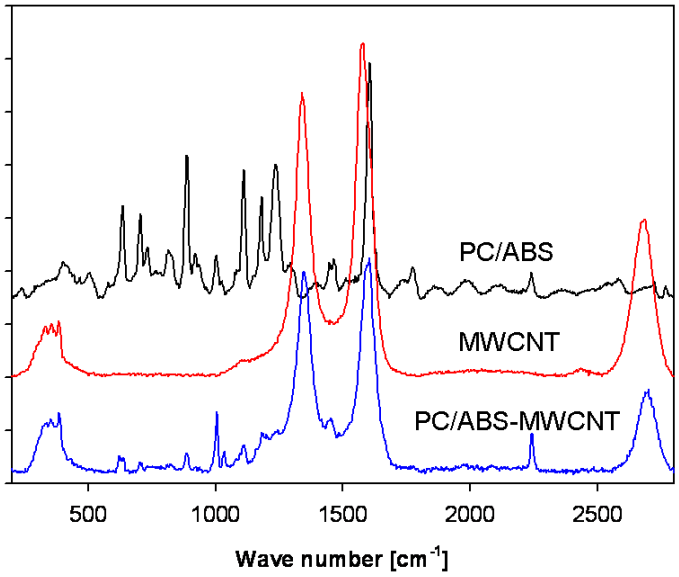

Figure 4.

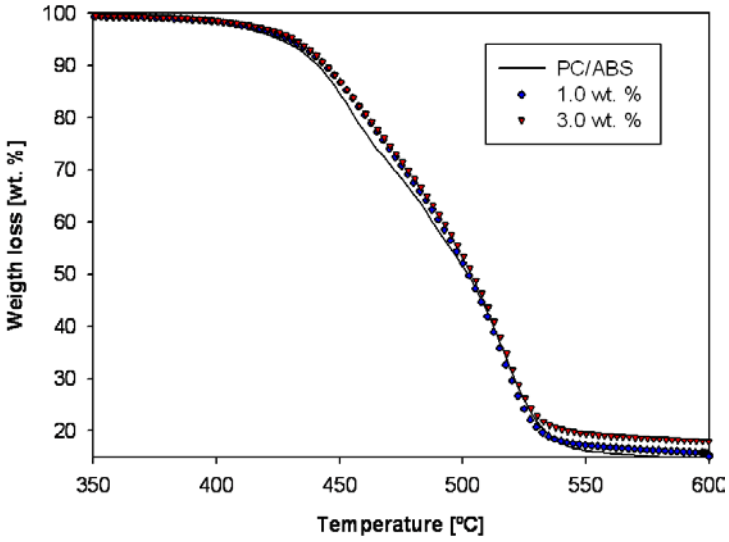

Figure 5.

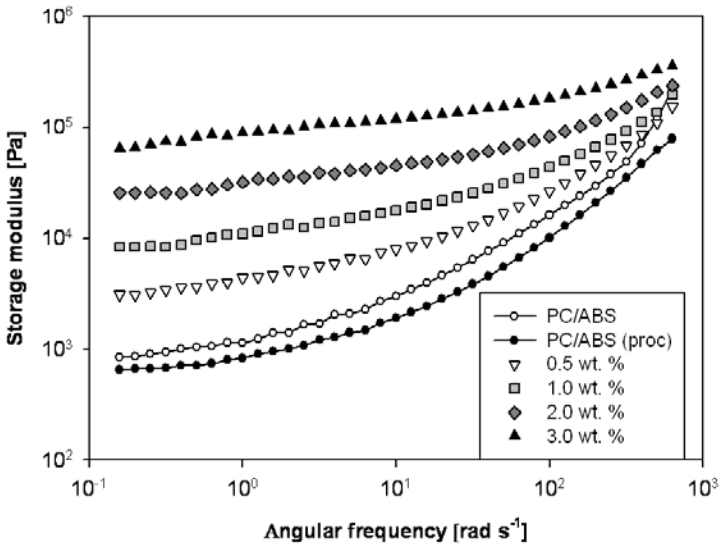

Figure 6.

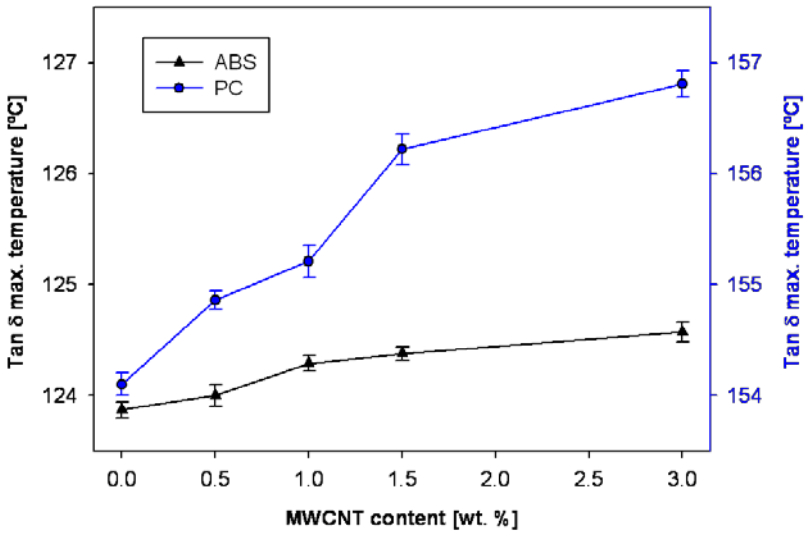

Figure 7.

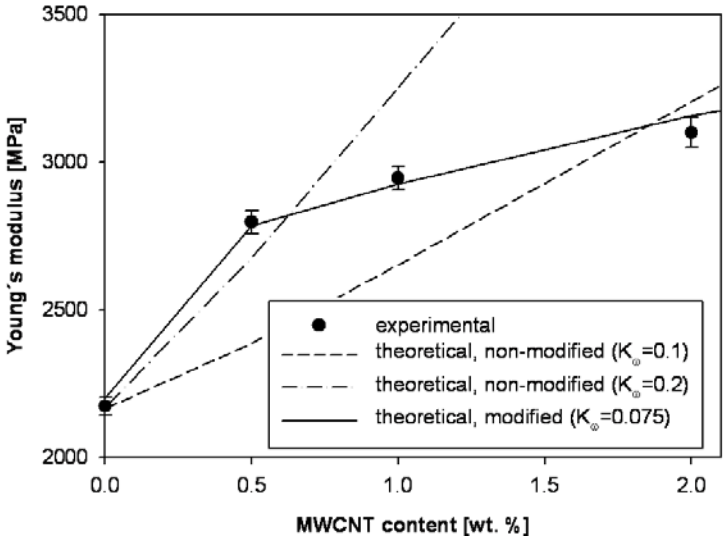

Figure 8.

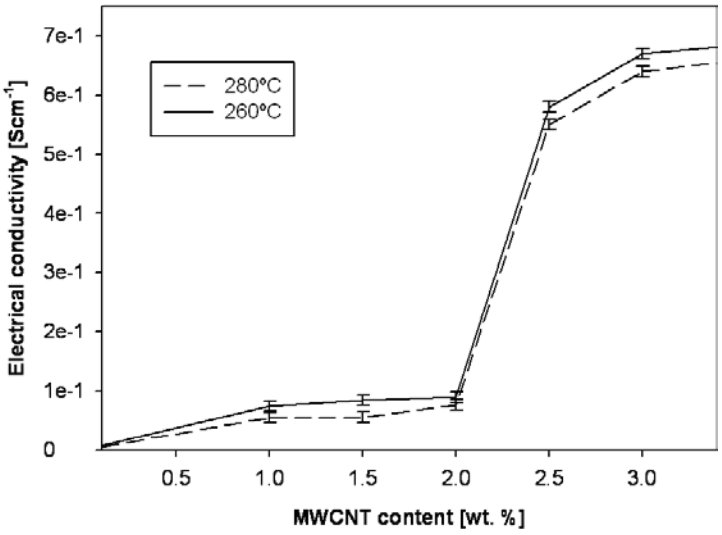

Figure 9.

Tables:

Table 1.

MWCNT [wt. %]	**ABS** $T_g^{(1)}$ **[°C]**	$\Delta C_p^{(2)}$ **[Jg^{-1}deg^{-1}]**	**w.d.$^{(3)}$ [°C]**	**PC** $T_g^{(1)}$ **[°C]**	$\Delta C_p^{(2)}$ **[Jg^{-1}deg^{-1}]**	**w.d.$^{(3)}$ [°C]**
0.0	119.2	0.082	452.2	141.0	0.115	514.0
0.5	114.8	0.062	454.6	142.0	0.118	515.1
1.0	114.6	0.058	457.7	142.6	0.139	516.3

2.0	114.2	0.048	457.9	143.0	0.159	517.5
3.0	113.9	0.043	458.2	143.4	0.165	518.3

(1) Glass transition temperature; (2) Change of heat capacity at glass transition; (3) Peak maximum of weight derivative obtained by TGA

Table 2.

MWCNT	**Mechanical properties**		
[wt. %]	**σ_y(1) [MPa]**	**ε_b(2) [%]**	**En(3) [J]**
0.0	44.8 (±1.0)	10.0 (±0.1)	806.0 (±12)
0.5	52.5 (±1.1)	9.3 (±0.5)	628.5 (±29)
1.0	56.1 (±1.3)	8.7 (±0.5)	440.5 (±32)
2.0	56.6 (±1.2)	7.5 (±0.6)	381.2 (±30)
3.0	57.0 (±1.4)	6.3 (±0.8)	344.7 (±25)
5.0	57.9 (±1.3)	4.6 (±0.6)	260.0 (±32)

(1) Stress at yield point; (2) Elongation at break; (3) Elastic strain energy